

Measurement of CP Asymmetries in $B^0 \rightarrow K_s^0 \pi^0 \pi^0$ Decays

The *BABAR* Collaboration

March 20, 2021

Abstract

We present a preliminary measurement of the time-dependent CP asymmetry for the neutral B -meson decay into the $CP = +1$ final state $K_s^0 \pi^0 \pi^0$, with $K_s^0 \rightarrow \pi^+ \pi^-$ and $\pi^0 \rightarrow \gamma \gamma$. We use a sample of approximately 227 million B -meson pairs recorded at the $\Upsilon(4S)$ resonance by the *BABAR* detector at the PEP-II B -Factory at SLAC. From a maximum likelihood fit we extract the mixing-induced CP -violation parameter $S_{K_s^0 \pi^0 \pi^0} = 0.84 \pm 0.71$ (stat) ± 0.08 (syst) and the direct CP -violation parameter $C_{K_s^0 \pi^0 \pi^0} = 0.27 \pm 0.52$ (stat) ± 0.13 (syst), where the first uncertainty is statistical and the second systematic.

Presented at the International Europhysics Conference On High-Energy Physics (HEP 2005),
7/21—7/27/2005, Lisbon, Portugal

Stanford Linear Accelerator Center, Stanford University, Stanford, CA 94309

Work supported in part by Department of Energy contract DE-AC03-76SF00515.

The BABAR Collaboration,

B. Aubert, R. Barate, D. Boutigny, F. Couderc, Y. Karyotakis, J. P. Lees, V. Poireau, V. Tisserand,
A. Zghiche

Laboratoire de Physique des Particules, F-74941 Annecy-le-Vieux, France

E. Grauges

IFAE, Universitat Autònoma de Barcelona, E-08193 Bellaterra, Barcelona, Spain

A. Palano, M. Pappagallo, A. Pompili

Università di Bari, Dipartimento di Fisica and INFN, I-70126 Bari, Italy

J. C. Chen, N. D. Qi, G. Rong, P. Wang, Y. S. Zhu

Institute of High Energy Physics, Beijing 100039, China

G. Eigen, I. Ofte, B. Stugu

University of Bergen, Institute of Physics, N-5007 Bergen, Norway

G. S. Abrams, M. Battaglia, A. B. Breon, D. N. Brown, J. Button-Shafer, R. N. Cahn, E. Charles,
C. T. Day, M. S. Gill, A. V. Gritsan, Y. Groysman, R. G. Jacobsen, R. W. Kadel, J. Kadyk, L. T. Kerth,
Yu. G. Kolomensky, G. Kukartsev, G. Lynch, L. M. Mir, P. J. Oddone, T. J. Orimoto, M. Pripstein,
N. A. Roe, M. T. Ronan, W. A. Wenzel

Lawrence Berkeley National Laboratory and University of California, Berkeley, California 94720, USA

M. Barrett, K. E. Ford, T. J. Harrison, A. J. Hart, C. M. Hawkes, S. E. Morgan, A. T. Watson

University of Birmingham, Birmingham, B15 2TT, United Kingdom

M. Fritsch, K. Goetzen, T. Held, H. Koch, B. Lewandowski, M. Pelizaeus, K. Peters, T. Schroeder,
M. Steinke

Ruhr Universität Bochum, Institut für Experimentalphysik 1, D-44780 Bochum, Germany

J. T. Boyd, J. P. Burke, N. Chevalier, W. N. Cottingham

University of Bristol, Bristol BS8 1TL, United Kingdom

T. Cuhadar-Donszelmann, B. G. Fulsom, C. Hearty, N. S. Knecht, T. S. Mattison, J. A. McKenna

University of British Columbia, Vancouver, British Columbia, Canada V6T 1Z1

A. Khan, P. Kyberd, M. Saleem, L. Teodorescu

Brunel University, Uxbridge, Middlesex UB8 3PH, United Kingdom

A. E. Blinov, V. E. Blinov, A. D. Bukin, V. P. Druzhinin, V. B. Golubev, E. A. Kravchenko,
A. P. Onuchin, S. I. Serebnyakov, Yu. I. Skovpen, E. P. Solodov, A. N. Yushkov

Budker Institute of Nuclear Physics, Novosibirsk 630090, Russia

D. Best, M. Bondioli, M. Bruinsma, M. Chao, S. Curry, I. Eschrich, D. Kirkby, A. J. Lankford, P. Lund,
M. Mandelkern, R. K. Mommsen, W. Roethel, D. P. Stoker

University of California at Irvine, Irvine, California 92697, USA

C. Buchanan, B. L. Hartfiel, A. J. R. Weinstein

University of California at Los Angeles, Los Angeles, California 90024, USA

S. D. Foulkes, J. W. Gary, O. Long, B. C. Shen, K. Wang, L. Zhang
University of California at Riverside, Riverside, California 92521, USA

D. del Re, H. K. Hadavand, E. J. Hill, D. B. MacFarlane, H. P. Paar, S. Rahatlou, V. Sharma
University of California at San Diego, La Jolla, California 92093, USA

J. W. Berryhill, C. Campagnari, A. Cunha, B. Dahmes, T. M. Hong, M. A. Mazur, J. D. Richman,
W. Verkerke
University of California at Santa Barbara, Santa Barbara, California 93106, USA

T. W. Beck, A. M. Eisner, C. J. Flacco, C. A. Heusch, J. Kroseberg, W. S. Lockman, G. Nesom, T. Schalk,
B. A. Schumm, A. Seiden, P. Spradlin, D. C. Williams, M. G. Wilson
University of California at Santa Cruz, Institute for Particle Physics, Santa Cruz, California 95064, USA

J. Albert, E. Chen, G. P. Dubois-Felsmann, A. Dvoretzki, D. G. Hitlin, I. Narsky, T. Piatenko,
F. C. Porter, A. Ryd, A. Samuel
California Institute of Technology, Pasadena, California 91125, USA

R. Andreassen, S. Jayatilleke, G. Mancinelli, B. T. Meadows, M. D. Sokoloff
University of Cincinnati, Cincinnati, Ohio 45221, USA

F. Blanc, P. Bloom, S. Chen, W. T. Ford, J. F. Hirschauer, A. Kreisel, U. Nauenberg, A. Olivas,
P. Rankin, W. O. Ruddick, J. G. Smith, K. A. Ulmer, S. R. Wagner, J. Zhang
University of Colorado, Boulder, Colorado 80309, USA

A. Chen, E. A. Eckhart, J. L. Harton, A. Soffer, W. H. Toki, R. J. Wilson, Q. Zeng
Colorado State University, Fort Collins, Colorado 80523, USA

D. Altenburg, E. Feltresi, A. Hauke, B. Spaan
Universität Dortmund, Institut für Physik, D-44221 Dortmund, Germany

T. Brandt, J. Brose, M. Dickopp, V. Klose, H. M. Lacker, R. Nogowski, S. Otto, A. Petzold, G. Schott,
J. Schubert, K. R. Schubert, R. Schwierz, J. E. Sundermann
Technische Universität Dresden, Institut für Kern- und Teilchenphysik, D-01062 Dresden, Germany

D. Bernard, G. R. Bonneaud, P. Grenier, S. Schrenk, Ch. Thiebaut, G. Vasileiadis, M. Verderi
Ecole Polytechnique, LLR, F-91128 Palaiseau, France

D. J. Bard, P. J. Clark, W. Gradl, F. Muheim, S. Playfer, Y. Xie
University of Edinburgh, Edinburgh EH9 3JZ, United Kingdom

M. Andreotti, V. Azzolini, D. Bettoni, C. Bozzi, R. Calabrese, G. Cibinetto, E. Luppi, M. Negrini,
L. Piemontese
Università di Ferrara, Dipartimento di Fisica and INFN, I-44100 Ferrara, Italy

F. Anulli, R. Baldini-Ferrolì, A. Calcaterra, R. de Sangro, G. Finocchiaro, P. Patteri, I. M. Peruzzi,¹
M. Piccolo, A. Zallo
Laboratori Nazionali di Frascati dell'INFN, I-00044 Frascati, Italy

¹Also with Università di Perugia, Dipartimento di Fisica, Perugia, Italy

A. Buzzo, R. Capra, R. Contri, M. Lo Vetere, M. Macri, M. R. Monge, S. Passaggio, C. Patrignani,
E. Robutti, A. Santroni, S. Tosi

Università di Genova, Dipartimento di Fisica and INFN, I-16146 Genova, Italy

G. Brandenburg, K. S. Chaisanguanthum, M. Morii, E. Won, J. Wu

Harvard University, Cambridge, Massachusetts 02138, USA

R. S. Dubitzky, U. Langenegger, J. Marks, S. Schenk, U. Uwer

Universität Heidelberg, Physikalisches Institut, Philosophenweg 12, D-69120 Heidelberg, Germany

W. Bhimji, D. A. Bowerman, P. D. Dauncey, U. Egede, R. L. Flack, J. R. Gaillard, G. W. Morton,
J. A. Nash, M. B. Nikolich, G. P. Taylor, W. P. Vazquez

Imperial College London, London, SW7 2AZ, United Kingdom

M. J. Charles, W. F. Mader, U. Mallik, A. K. Mohapatra

University of Iowa, Iowa City, Iowa 52242, USA

J. Cochran, H. B. Crawley, V. Eyges, W. T. Meyer, S. Prell, E. I. Rosenberg, A. E. Rubin, J. Yi

Iowa State University, Ames, Iowa 50011-3160, USA

N. Arnaud, M. Davier, X. Giroux, G. Grosdidier, A. Höcker, F. Le Diberder, V. Lepeltier, A. M. Lutz,
A. Oyanguren, T. C. Petersen, M. Pierini, S. Plaszczynski, S. Rodier, P. Roudeau, M. H. Schune,
A. Stocchi, G. Wormser

Laboratoire de l'Accélérateur Linéaire, F-91898 Orsay, France

C. H. Cheng, D. J. Lange, M. C. Simani, D. M. Wright

Lawrence Livermore National Laboratory, Livermore, California 94550, USA

A. J. Bevan, C. A. Chavez, I. J. Forster, J. R. Fry, E. Gabathuler, R. Gamet, K. A. George,
D. E. Hutchcroft, R. J. Parry, D. J. Payne, K. C. Schofield, C. Touramanis

University of Liverpool, Liverpool L69 7ZE, United Kingdom

C. M. Cormack, F. Di Lodovico, W. Menges, R. Sacco

Queen Mary, University of London, E1 4NS, United Kingdom

C. L. Brown, G. Cowan, H. U. Flaecher, M. G. Green, D. A. Hopkins, P. S. Jackson, T. R. McMahon,
S. Ricciardi, F. Salvatore

University of London, Royal Holloway and Bedford New College, Egham, Surrey TW20 0EX, United Kingdom

D. Brown, C. L. Davis

University of Louisville, Louisville, Kentucky 40292, USA

J. Allison, N. R. Barlow, R. J. Barlow, C. L. Edgar, M. C. Hodgkinson, M. P. Kelly, G. D. Lafferty,
M. T. Naisbit, J. C. Williams

University of Manchester, Manchester M13 9PL, United Kingdom

C. Chen, W. D. Hulsbergen, A. Jawahery, D. Kovalskyi, C. K. Lae, D. A. Roberts, G. Simi

University of Maryland, College Park, Maryland 20742, USA

G. Blaylock, C. Dallapiccola, S. S. Hertzbach, R. Kofler, V. B. Koptchev, X. Li, T. B. Moore, S. Saremi,
H. Staengle, S. Willocq

University of Massachusetts, Amherst, Massachusetts 01003, USA

R. Cowan, K. Koeneke, G. Sciolla, S. J. Sekula, M. Spitznagel, F. Taylor, R. K. Yamamoto
*Massachusetts Institute of Technology, Laboratory for Nuclear Science, Cambridge, Massachusetts 02139,
USA*

H. Kim, P. M. Patel, S. H. Robertson
McGill University, Montréal, Quebec, Canada H3A 2T8

A. Lazzaro, V. Lombardo, F. Palombo
Università di Milano, Dipartimento di Fisica and INFN, I-20133 Milano, Italy

J. M. Bauer, L. Cremaldi, V. Eschenburg, R. Godang, R. Kroeger, J. Reidy, D. A. Sanders, D. J. Summers,
H. W. Zhao

University of Mississippi, University, Mississippi 38677, USA

S. Brunet, D. Côté, P. Taras, B. Viaud
Université de Montréal, Laboratoire René J. A. Lévêque, Montréal, Quebec, Canada H3C 3J7

H. Nicholson
Mount Holyoke College, South Hadley, Massachusetts 01075, USA

N. Cavallo,² G. De Nardo, F. Fabozzi,² C. Gatto, L. Lista, D. Monorchio, P. Paolucci, D. Piccolo,
C. Sciacca

Università di Napoli Federico II, Dipartimento di Scienze Fisiche and INFN, I-80126, Napoli, Italy

M. Baak, H. Bulten, G. Raven, H. L. Snoek, L. Wilden
*NIKHEF, National Institute for Nuclear Physics and High Energy Physics, NL-1009 DB Amsterdam, The
Netherlands*

C. P. Jessop, J. M. LoSecco
University of Notre Dame, Notre Dame, Indiana 46556, USA

T. Allmendinger, G. Benelli, K. K. Gan, K. Honscheid, D. Hufnagel, P. D. Jackson, H. Kagan, R. Kass,
T. Pulliam, A. M. Rahimi, R. Ter-Antonyan, Q. K. Wong

Ohio State University, Columbus, Ohio 43210, USA

J. Brau, R. Frey, O. Igonkina, M. Lu, C. T. Potter, N. B. Sinev, D. Strom, J. Strube, E. Torrence
University of Oregon, Eugene, Oregon 97403, USA

F. Galeazzi, M. Margoni, M. Morandin, M. Posocco, M. Rotondo, F. Simonetto, R. Stroili, C. Voci
Università di Padova, Dipartimento di Fisica and INFN, I-35131 Padova, Italy

M. Benayoun, H. Briand, J. Chauveau, P. David, L. Del Buono, Ch. de la Vaissière, O. Hamon,
M. J. J. John, Ph. Leruste, J. Malclès, J. Ocariz, M. Pivk, L. Roos, G. Therin
*Universités Paris VI et VII, Laboratoire de Physique Nucléaire et de Hautes Energies, F-75252 Paris,
France*

²Also with Università della Basilicata, Potenza, Italy

P. K. Behera, L. Gladney, Q. H. Guo, J. Panetta
University of Pennsylvania, Philadelphia, Pennsylvania 19104, USA

M. Biasini, R. Covarelli, S. Pacetti, M. Pioppi
Università di Perugia, Dipartimento di Fisica and INFN, I-06100 Perugia, Italy

C. Angelini, G. Batignani, S. Bettarini, F. Bucci, G. Calderini, M. Carpinelli, R. Cenci, F. Forti,
M. A. Giorgi, A. Lusiani, G. Marchiori, M. Morganti, N. Neri, E. Paoloni, M. Rama, G. Rizzo, J. Walsh
Università di Pisa, Dipartimento di Fisica, Scuola Normale Superiore and INFN, I-56127 Pisa, Italy

M. Haire, D. Judd, D. E. Wagoner
Prairie View A&M University, Prairie View, Texas 77446, USA

J. Biesiada, N. Danielson, P. Elmer, Y. P. Lau, C. Lu, J. Olsen, A. J. S. Smith, A. V. Telnov
Princeton University, Princeton, New Jersey 08544, USA

E. Baracchini, F. Bellini, G. Cavoto, A. D'Orazio, E. Di Marco, R. Faccini, F. Ferrarotto, F. Ferroni,
M. Gaspero, L. Li Gioi, M. A. Mazzoni, S. Morganti, G. Piredda, F. Polci, F. Safai Tehrani, C. Voena
Università di Roma La Sapienza, Dipartimento di Fisica and INFN, I-00185 Roma, Italy

H. Schröder, G. Wagner, R. Waldi
Universität Rostock, D-18051 Rostock, Germany

T. Adye, N. De Groot, B. Franek, G. P. Gopal, E. O. Olaiya, F. F. Wilson
Rutherford Appleton Laboratory, Chilton, Didcot, Oxon, OX11 0QX, United Kingdom

R. Aleksan, S. Emery, A. Gaidot, S. F. Ganzhur, P.-F. Giraud, G. Graziani, G. Hamel de Monchenault,
W. Kozanecki, M. Legendre, G. W. London, B. Mayer, G. Vasseur, Ch. Yèche, M. Zito
DSM/Dapnia, CEA/Saclay, F-91191 Gif-sur-Yvette, France

M. V. Purohit, A. W. Weidemann, J. R. Wilson, F. X. Yumiceva
University of South Carolina, Columbia, South Carolina 29208, USA

T. Abe, M. T. Allen, D. Aston, N. van Bakel, R. Bartoldus, N. Berger, A. M. Boyarski, O. L. Buchmueller,
R. Claus, J. P. Coleman, M. R. Convery, M. Cristinziani, J. C. Dingfelder, D. Dong, J. Dorfan, D. Dujmic,
W. Dunwoodie, S. Fan, R. C. Field, T. Glanzman, S. J. Gowdy, T. Hadig, V. Halyo, C. Hast, T. Hryn'ova,
W. R. Innes, M. H. Kelsey, P. Kim, M. L. Kocian, D. W. G. S. Leith, J. Libby, S. Luitz, V. Luth,
H. L. Lynch, H. Marsiske, R. Messner, D. R. Muller, C. P. O'Grady, V. E. Ozcan, A. Perazzo, M. Perl,
B. N. Ratcliff, A. Roodman, A. A. Salnikov, R. H. Schindler, J. Schwiening, A. Snyder, J. Stelzer, D. Su,
M. K. Sullivan, K. Suzuki, S. Swain, J. M. Thompson, J. Va'vra, M. Weaver, W. J. Wisniewski,
M. Wittgen, D. H. Wright, A. K. Yarritu, K. Yi, C. C. Young
Stanford Linear Accelerator Center, Stanford, California 94309, USA

P. R. Burchat, A. J. Edwards, S. A. Majewski, B. A. Petersen, C. Roat
Stanford University, Stanford, California 94305-4060, USA

M. Ahmed, S. Ahmed, M. S. Alam, J. A. Ernst, M. A. Saeed, F. R. Wappler, S. B. Zain
State University of New York, Albany, New York 12222, USA

W. Bugg, M. Krishnamurthy, S. M. Spanier
University of Tennessee, Knoxville, Tennessee 37996, USA

R. Eckmann, J. L. Ritchie, A. Satpathy, R. F. Schwitters
University of Texas at Austin, Austin, Texas 78712, USA

J. M. Izen, I. Kitayama, X. C. Lou, S. Ye
University of Texas at Dallas, Richardson, Texas 75083, USA

F. Bianchi, M. Bona, F. Gallo, D. Gamba
Università di Torino, Dipartimento di Fisica Sperimentale and INFN, I-10125 Torino, Italy

M. Bomben, L. Bosisio, C. Cartaro, F. Cossutti, G. Della Ricca, S. Dittongo, S. Grancagnolo, L. Lanceri,
L. Vitale
Università di Trieste, Dipartimento di Fisica and INFN, I-34127 Trieste, Italy

F. Martinez-Vidal
IFIC, Universitat de Valencia-CSIC, E-46071 Valencia, Spain

R. S. Panvini³
Vanderbilt University, Nashville, Tennessee 37235, USA

Sw. Banerjee, B. Bhuyan, C. M. Brown, D. Fortin, K. Hamano, R. Kowalewski, J. M. Roney, R. J. Sobie
University of Victoria, Victoria, British Columbia, Canada V8W 3P6

J. J. Back, P. F. Harrison, T. E. Latham, G. B. Mohanty
Department of Physics, University of Warwick, Coventry CV4 7AL, United Kingdom

H. R. Band, X. Chen, B. Cheng, S. Dasu, M. Datta, A. M. Eichenbaum, K. T. Flood, M. Graham,
J. J. Hollar, J. R. Johnson, P. E. Kutter, H. Li, R. Liu, B. Mellado, A. Mihalyi, Y. Pan, R. Prepost,
P. Tan, J. H. von Wimmersperg-Toeller, S. L. Wu, Z. Yu
University of Wisconsin, Madison, Wisconsin 53706, USA

H. Neal
Yale University, New Haven, Connecticut 06511, USA

³Deceased

1 INTRODUCTION

CP violation effects in decays of B mesons that are dominated by $b \rightarrow s\bar{q}q$ transitions, where $q = u, d, s$, are potentially sensitive to contributions from physics beyond the Standard Model [1]. The B -factory experiments have explored time-dependent CP -violating (CPV) asymmetries in several such decays [2], including $B^0 \rightarrow \phi K^0$ [3, 4], $B^0 \rightarrow K_s^0 K_s^0 K_s^0$ [5], $B^0 \rightarrow \eta' K_s^0$ [3, 6], $B^0 \rightarrow K^+ K^- K_s^0$ [3, 7], $B^0 \rightarrow f_0(980) K_s^0$ [8] and $B^0 \rightarrow K_s^0 \pi^0$ [9]. Within the Standard Model the asymmetry in these decays is expected to be consistent with the asymmetry in $b \rightarrow \bar{c}s$ decays, such as $B^0 \rightarrow J/\psi K_s^0$, where the CPV asymmetry occurs due to a phase difference between mixing and decay amplitudes. These comparisons must take into account contributions of other amplitudes with different weak-interaction phases within the Standard Model. A major goal of the B -factory experiments is to reduce the experimental uncertainties of these measurements and to add more decay modes in order to improve the sensitivity to beyond-the-Standard-Model effects.

In this letter we present a preliminary measurement of the CPV asymmetry in the decay $B^0 \rightarrow K_s^0 \pi^0 \pi^0$, using data collected with the $BABAR$ detector at the PEP-II asymmetric-energy e^+e^- collider. In the Standard Model this decay is dominated by the $b \rightarrow s\bar{q}q$ amplitude, with $q = u, d$. A possible contribution from a tree-level $b \rightarrow u\bar{u}s$ amplitude is doubly Cabibbo-suppressed with respect to the leading gluonic penguin diagram.

The $K_s^0 \pi^0 \pi^0$ final state is a CP -even eigenstate, regardless of any resonant substructure [10]. In the Standard Model we expect $S_{K_s^0 \pi^0 \pi^0} \simeq -\sin 2\beta$ and $C_{K_s^0 \pi^0 \pi^0} \simeq 0$. The angle β is defined as $\beta = \arg(-V_{cd}V_{cb}^*/V_{td}V_{tb}^*)$ and V_{ij} are the elements of the CKM matrix [11]. A significant measurement of CP violation in this channel alone in comparison to other penguin modes constrains certain extensions of the Standard Model [12].

2 THE $BABAR$ DETECTOR AND DATASET

The data in this analysis were collected with the $BABAR$ detector [13] at the PEP-II asymmetric e^+e^- collider [14]. A sample of 226.6 ± 2.5 million $B\bar{B}$ pairs was recorded at the $\mathcal{T}(4S)$ resonance (center-of-mass energy $\sqrt{s} = 10.58$ GeV). The $BABAR$ detector is described in detail elsewhere [13]. Charged particles are detected and their momenta measured by the combination of a silicon vertex tracker (SVT), consisting of five layers of double-sided detectors, and a 40-layer central drift chamber, both operating in the 1.5 T magnetic field of a solenoid. Charged-particle identification (PID) is provided by the average energy loss in the tracking devices and by an internally reflecting ring-imaging Cherenkov detector (DIRC) covering the central region. Photons and electrons are detected by an electromagnetic calorimeter composed of 6580 CsI(Tl) crystals; the typical resolution for the π^0 signal in the $\gamma\gamma$ invariant mass spectrum is better than 7 MeV/ c^2 .

3 ANALYSIS METHOD

In the decay $B^0 \rightarrow K_s^0 \pi^0 \pi^0$, which has no charged tracks originating from the B^0 decay vertex, we rely on the technique recently developed to reconstruct the B^0 vertex in $B^0 \rightarrow K_s^0 \pi^0$ decays (described in detail below) [9]. From a candidate $B\bar{B}$ pair we reconstruct a B^0 decaying into the CP eigenstate $K_s^0 \pi^0 \pi^0$ (B_{CP}). We also reconstruct the vertex of the other B meson (B_{tag}) and identify its flavor. The difference $\Delta t \equiv t_{CP} - t_{\text{tag}}$ of the proper decay times is obtained from the measured distance between the B_{CP} and B_{tag} decay vertices and from the boost ($\beta\gamma = 0.56$) of the

e^+e^- system. The Δt distribution is given by:

$$\mathcal{P}_{\pm}(\Delta t) = \frac{e^{-|\Delta t|/\tau}}{4\tau} [1 \mp \Delta w \pm (1 - 2w)(S \sin(\Delta m_d \Delta t) - C \cos(\Delta m_d \Delta t))]. \quad (1)$$

The upper (lower) sign denotes a decay accompanied by a B^0 (\bar{B}^0) tag, τ is the mean B^0 lifetime, Δm_d is the mixing frequency, and the mistag parameters w and Δw are the average and difference, respectively, of the probabilities that a true B^0 is incorrectly tagged as a \bar{B}^0 or vice versa. The tagging algorithm [15] has seven mutually exclusive tagging categories of differing purities (including one for untagged events that we retain only for yield determinations). The analyzing power, defined as efficiency times $(1 - 2w)^2$ summed over all categories, is $(30.5 \pm 0.6)\%$, as determined from a large sample of B -decays to fully reconstructed flavor eigenstates (B_{flav}).

We search for $B^0 \rightarrow K_S^0 \pi^0 \pi^0$ decays in $B\bar{B}$ candidate events selected using charged-particle multiplicity and event topology [16]. We reconstruct $K_S^0 \rightarrow \pi^+ \pi^-$ candidates from pairs of oppositely charged tracks. The two-track combinations must form a vertex with a χ^2 probability greater than 0.001 and a $\pi^+ \pi^-$ invariant mass within 11.2 MeV/ c^2 of the nominal K_S^0 mass [17]. We form $\pi^0 \rightarrow \gamma\gamma$ candidates from pairs of photon candidates in the EMC, each of which is isolated from any charged tracks, carries a minimum energy of 30 MeV, and has the expected lateral shower shape. Candidates for $B^0 \rightarrow K_S^0 \pi^0 \pi^0$ are formed from $K_S^0 \pi^0 \pi^0$ combinations and constrained to originate from the e^+e^- interaction point using a geometric fit. We require that the χ^2 consistency of the fit, which has one degree of freedom, be greater than 0.001. We extract the K_S^0 decay length $L_{K_S^0}$ and the $\pi^0 \rightarrow \gamma\gamma$ invariant mass from this fit and require $110 < m_{\gamma\gamma} < 160$ MeV/ c^2 and $L_{K_S^0}$ greater than 5 times its uncertainty. The cosine of the angle between the direction of the decay photon in the center-of-mass system of the mother π^0 and the π^0 flight direction must be less than 0.92.

We extract the signal yield, S and C from an unbinned extended maximum likelihood fit where we parameterize the distributions of several kinematic and topological variables for signal and background events in terms of probability density functions (PDFs).

For each B candidate we compute two kinematic variables, the energy difference $\Delta E = E_B^* - \frac{1}{2}\sqrt{s}$ and the beam-energy-substituted mass $m_{\text{ES}} = \sqrt{(\frac{1}{2}s + \vec{p}_0 \cdot \vec{p}_B)^2 / E_0^2 - p_B^2}$ [13], where s is the center-of-mass energy squared. The subscripts 0 and B refer to the initial $\Upsilon(4S)$ and the B_{CP} candidate, respectively, and the asterisk denotes the center-of-mass frame. For signal events, ΔE is expected to peak at zero and m_{ES} at the known B mass. From a detailed simulation we expect a signal resolution of about 3.6 MeV/ c^2 in m_{ES} and 45 MeV in ΔE . Both distributions exhibit a low-side tail due to the response of the EMC to photons. We remove a small dependence of the signal ΔE resolution on the location in the $K_S^0 \pi^0 \pi^0$ Dalitz plot by using $\Delta E / \sigma(\Delta E)$ instead of ΔE , where $\sigma(\Delta E)$ is the measured uncertainty in ΔE . We select candidates with $m_{\text{ES}} > 5.20$ GeV/ c^2 and $-5 < \Delta E / \sigma(\Delta E) < 2$. To suppress other B decays we also require $-0.25 < \Delta E < 0.1$ GeV, which does not affect the signal $\Delta E / \sigma(\Delta E)$ distribution.

The background B candidates come primarily from random combinations of K_S^0 and neutral pions produced in events of the type $e^+e^- \rightarrow q\bar{q}$, where $q = u, d, s, c$ (continuum). Background from $B\bar{B}$ events may occur either in charmless decays $B^0 \rightarrow K_S^0 X$, or from decays where the K_S^0 is from an intermediate charmed particle. The shapes of event variable distributions are obtained from signal and background Monte Carlo (MC) samples and high statistics data control samples. In m_{ES} , the charmless B background exhibits a broad enhancement near the B -meson mass while

other B background distributions show no peaking. In $\Delta E/\sigma(\Delta E)$, B backgrounds in general show no clustering.

In continuum events, particles appear mostly in two jets. This topology can be characterized with several variables computed in the $\Upsilon(4S)$ frame. One such quantity is the angle θ_T between the thrust axis of the B_{CP} candidate and the thrust axis formed from the other charged and neutral particles in the event, where the thrust axis is defined as the axis that maximizes the sum of the magnitudes of the longitudinal momenta. This angle is small for continuum events and uniformly distributed for true $B\bar{B}$ events. With the requirement $|\cos\theta_T| < 0.9$ we suppress background by a factor of three while retaining 90% of the signal. We also use the angle θ_B between the B_{CP} momentum and the beam axis, and the sum of the momenta p_i of the other charged and neutral particles in the event weighted by the Legendre polynomials $L_0(\theta_i)$ and $L_2(\theta_i)$ where θ_i is the angle between the momentum of particle i and the thrust axis of the B_{CP} candidate. We combine these three variables in a neural net (NN) that is trained and evaluated [18] on different subsets of simulated signal and continuum events and on data taken about 40 MeV below the nominal center-of-mass energy. The NN has two hidden layers with 4 neurons each. The NN output is divided into 10 consecutive intervals, chosen such that they are uniformly populated by the signal events; the PDF is modeled as a parametric step function [19] whose parameters are the heights of each bin. Since the parent distribution for the NN output is unknown any assumed functional form will suffer a systematic uncertainty due to the choice of the function.

We suppress background from other B decays by excluding several invariant mass intervals: $m(K_S^0\pi^0) > 4.8$ GeV/ c^2 eliminates $B^0 \rightarrow K_S^0\pi^0$, $1.75 < m(K_S^0\pi^0) < 1.99$ GeV/ c^2 reduces $B^0 \rightarrow \bar{D}^0\pi^0$ to fewer than 10 expected candidates, $m(\pi^0\pi^0) < 0.6$ GeV/ c^2 removes ηK_S^0 and $\eta' K_S^0$, and $3.2 < m(\pi^0\pi^0) < 3.5$ GeV/ c^2 removes $\chi_{c0} K_S^0$ and $\chi_{c2} K_S^0$ candidates.

From MC simulation we expect more than one candidate in 13% of the signal candidate events. Because the number of multiple K_S^0 candidates is negligible (less than 0.1%), we select the candidate whose two reconstructed π^0 masses are closest to the expected value. The signal reconstruction efficiency is about 15%.

For each $B^0 \rightarrow K_S^0\pi^0\pi^0$ candidate we examine the remaining tracks in the event to determine the decay vertex position and the flavor of B_{tag} . We parameterize the performance of the tagging algorithm in a data sample (B_{flav}) of fully reconstructed $B^0 \rightarrow D^{(*)-}\pi^+/\rho^+/a_1^+$ decays. For the continuum background, the fraction of events tagged in category k , ϵ_k , is extracted from a fit to the data. The B_{tag} vertex is reconstructed inclusively from the remaining charged particles in the event [16].

To reconstruct the B_{CP} vertex from the single K_S^0 trajectory we exploit the knowledge of the average interaction point (IP), which is determined every 10 minutes from the spatial distribution of vertices from two-track events. The uncertainty on the IP position, which follows from the size of the interaction region, is about 150 μm horizontally and 4 μm vertically. We compute Δt and its uncertainty from a geometric fit [20] to the $\Upsilon(4S) \rightarrow B^0\bar{B}^0$ system that takes this IP constraint into account. We further improve the sensitivity to Δt by constraining the sum of the two B decay times ($t_{CP} + t_{\text{tag}}$) to be equal to $2\tau_{B^0}$ with an uncertainty of $\sqrt{2}\tau_{B^0}$, which effectively constrains the two vertices to be near the $\Upsilon(4S)$ line of flight. This procedure provides an unbiased estimate of Δt . The extraction of Δt with the IP-constrained fit has been extensively tested on large samples of simulated $B^0 \rightarrow K_S^0\pi^0\pi^0$ decays with different values of S and C , and in data [9].

The per-event estimate of the uncertainty on Δt reflects the strong dependence of the Δt resolution on the K_S^0 flight direction and on the number of SVT layers traversed by the K_S^0 decay daughters. In about 70% of the events both pion tracks are reconstructed from at least 4 SVT hits,

leading to sufficient resolution for the time-dependent measurement. The average Δt resolution in these events is about 1.0 ps. For events that fail this criterion or for which $\sigma(\Delta t) > 2.5$ ps or $\Delta t > 20$ ps, the Δt information is not used. However, since C can also be extracted from flavor tagging information alone, these events still contribute to the measurement of C .

By exploiting regions in data that are dominated by background, and simulated events for the signal, we have verified that with our selection the observables are sufficiently independent that we can construct the likelihood from the product of one-dimensional PDFs, apart from the signal m_{ES} and $\Delta E/\sigma(\Delta E)$ which are correlated away from their mean signal positions and for which we use a two-dimensional PDF derived from a smoothed, simulated distribution. We obtain the PDF for the Δt of signal events from the convolution of Eq.(1) with a resolution function $\mathcal{R}(\delta t \equiv \Delta t - \Delta t_{\text{true}}, \sigma_{\Delta t})$. The resolution function is parameterized as the sum of two Gaussians with a width proportional to the reconstructed $\sigma_{\Delta t}$, and a third Gaussian with a fixed width of 8 ps [16]. The first two Gaussian distributions have a non-zero mean, proportional to $\sigma_{\Delta t}$, to account for the charm decays on the B_{tag} side. We have verified in simulation that the parameters of $\mathcal{R}(\delta t, \sigma_{\Delta t})$ for $B^0 \rightarrow K_S^0 \pi^0 \pi^0$ events are similar to those obtained from the B_{flav} sample, even though the distributions of $\sigma_{\Delta t}$ differ considerably. We therefore extract these parameters from a fit to the B_{flav} sample. We use the same resolution function for background from other charmless B decays. The Δt distributions for background from B decays into open charm final states and continuum consist of a prompt component and a non-prompt component, and the resolution function has the same functional form as used for signal events. The parameters for the Δt PDF of the open-charm background are determined from MC simulation, while for the continuum they are varied in the fit to data.

4 MAXIMUM LIKELIHOOD FIT

We subdivide the data into the tagging categories k , events with and without Δt information (set I and II), and those located in the inside or outside region of the Dalitz plot (*inside* or *outside*). The latter accounts for the higher contribution and different characteristics of continuum background near the Dalitz plot boundary. We define the quantity $\delta = \min(m_{12}^2, m_{13}^2, m_{23}^2)$, where m_{ij} is the invariant mass of the B decay daughters i and j combined. It corresponds to the distance of an event in the Dalitz plot to the nearest Dalitz plot boundary in the limit of massless daughters. We split the data at $\delta = 3.5 \text{ GeV}^2/c^4$. We maximize the logarithm of the extended likelihood $\mathcal{L} = e^{(N_S + N_B)} \cdot \prod_k l_k$ with N_S and $N_B (= \sum_B n_B)$ the total signal and background yields, respectively. The likelihood in each tagging category k (with tagging fraction ϵ_k) is given as:

$$\begin{aligned}
l_k = & \prod_j^{NI \text{ outside } k} \left[N_S \epsilon_k^S f_g^S f_{out}^S P_{k,j}^S + \sum_B n_B \epsilon_k^B f_g^B f_{out}^B P_{k,out,j}^B \right] \times \\
& \prod_j^{NI \text{ inside } k} \left[N_S \epsilon_k^S f_g^S (1 - f_{out}^S) P_{k,j}^S + \sum_B n_B \epsilon_k^B f_g^B (1 - f_{out}^B) P_{k,in,j}^B \right] \times \\
& \prod_j^{NII \text{ outside } k} \left[N_S \epsilon_k^S (1 - f_g^S) f_{out}^S Q_{k,j}^S + \sum_B n_B \epsilon_k^B (1 - f_g^B) f_{out}^B Q_{k,out,j}^B \right] \times \\
& \prod_j^{NII \text{ inside } k} \left[N_S \epsilon_k^S (1 - f_g^S) (1 - f_{out}^S) Q_{k,j}^S + \sum_B n_B \epsilon_k^B (1 - f_g^B) (1 - f_{out}^B) Q_{k,in,j}^B \right]. \quad (2)
\end{aligned}$$

The probabilities P^S (Q^S) and P^B (Q^B) for each measurement j are the products of PDFs for signal (S) and background (B) classes: $P_{k,j} = PDF(m_{ESj}, \Delta E/\sigma(\Delta E)_j) \cdot PDF(NN_j) \cdot PDF(\Delta t_j, \sigma(\Delta t)_j, \text{tag}_{k,j}, k_j)$, where for the background $PDF(m_{ESj}, \Delta E/\sigma(\Delta E)_j) = PDF(m_{ESj}) \cdot PDF(\Delta E/\sigma(\Delta E)_j)$. The probabilities Q do not depend on Δt and $\sigma(\Delta t)$ and are used to extract C from the yields. The fractions of events with Δt information for signal and background are denoted by f_g^S and f_g^B , respectively, and fractions of events in the outside Dalitz plot region by f_{out}^S and f_{out}^B . For about 22% of our signal B candidates one or two of the π^0 decay photons associated with B_{CP} originate from the B_{tag} . According to Monte Carlo simulation studies in these cross-feed events we expect to measure the same S and C as in the correctly reconstructed signal (*true*) since the contribution of the π^0 to the Δt measurement is marginal. To account for differences in the PDF distributions for the signal probabilities P^S (Q^S) we use: $P = f_{cf}P_{cf} + (1 - f_{cf})P_{true}$. The fraction of cross-feed events, f_{cf} , is fixed to the value obtained from the simulation. Parameters of signal PDFs are the same for the different Dalitz plot regions. The PDFs for B backgrounds are identical for the Dalitz inside and outside regions. The tagging fractions for the signal and the B decay backgrounds are the same; continuum background has different ϵ_k^B . The good fractions f_g^S and f_g^B and the outside fractions f_{out}^S and f_{out}^B for continuum are varied in the fit, while these fractions for charm and charmless B backgrounds are determined from Monte Carlo simulations. The fit was tested with both a parameterized simulation of a large number of data-sized experiments and a full detector simulation.

5 PHYSICS RESULTS

The central values of S and C were hidden until the analysis was complete. From a data sample of 33,058 $B^0 \rightarrow K_S^0 \pi^0 \pi^0$ candidates, we find $N_S = 117 \pm 27$ signal decays with $S_{K_S^0 \pi^0 \pi^0} = 0.84 \pm 0.71$ (stat) ± 0.08 (syst) and $C_{K_S^0 \pi^0 \pi^0} = 0.27 \pm 0.52$ (stat) ± 0.13 (syst). The linear correlation coefficient between the two CP parameters is 2%. The yield of charmless B background is consistent with zero. Figure 1 shows the distributions of the event variables m_{ES} , $\Delta E/\sigma(\Delta E)$, and NN , and Fig. 2 shows the Δt distributions for the B^0 - and the \bar{B}^0 -tagged subsets with the raw asymmetry $[N_{B^0} - N_{\bar{B}^0}]/[N_{B^0} + N_{\bar{B}^0}]$. The N_{B^0} ($N_{\bar{B}^0}$) is the number of B^0 (\bar{B}^0)-tagged events. In all plots data are displayed together with the result from the fit after applying a requirement on the ratio of signal likelihood to signal-plus-background likelihood (computed without the variable plotted) to reduce the background.

6 SYSTEMATIC STUDIES

We consider systematic uncertainties listed in Table 1. These include the uncertainties in the parameterization of PDFs for signal and backgrounds which were evaluated by varying parameters within one standard deviation or using alternative shape functions. The largest uncertainty for C is caused by the NN shape for continuum inside the Dalitz plot ($\sigma(C) = 0.10$) and for S from the 2-D parameterization ($\sigma(S) = 0.04$). We consider uncertainties in the background fractions and CP asymmetry in the charmless B background, the parameterization of the Δt resolution function and the vertex finding method, knowledge of the event-by-event beam spot position, imprecision in the SVT alignment, and the possible interference between the suppressed $\bar{b} \rightarrow \bar{u}\bar{d}$ amplitude with the favored $b \rightarrow \bar{u}d$ amplitude for tag-side B -decays [21]. We fix $\tau_{B^0} = 1.532$ ps and $\Delta m_d = 0.505$ ps⁻¹ and vary them by one standard deviation [17]. We correct for the small fit bias which is determined

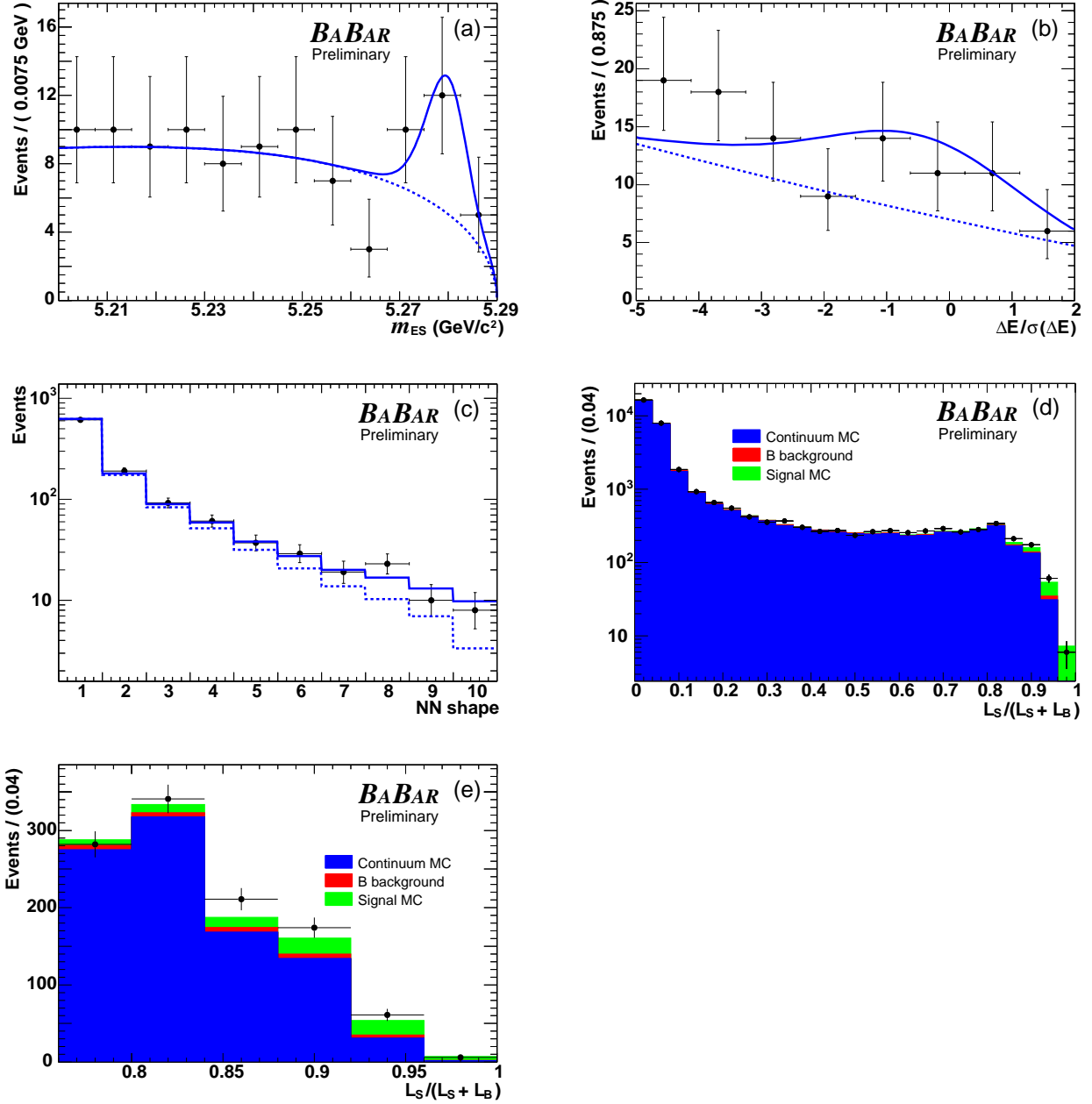


Figure 1: Distribution of the event variables (a) m_{ES} , (b) $\Delta E/\sigma(\Delta E)$, and (c) NN output in 10 bins after reconstruction and a requirement on the ratio of signal likelihood to the signal-plus-background likelihood, calculated without the plotted variable. The solid line represents the fit result for the total event yield and the dotted line for the total background. Plot (d) shows the ratio of the signal likelihood to signal-plus-background likelihood with all variables included, data (dots) with the fit result superimposed. Plot (e) shows the same quantity as (d) close to one and with a linear scale.

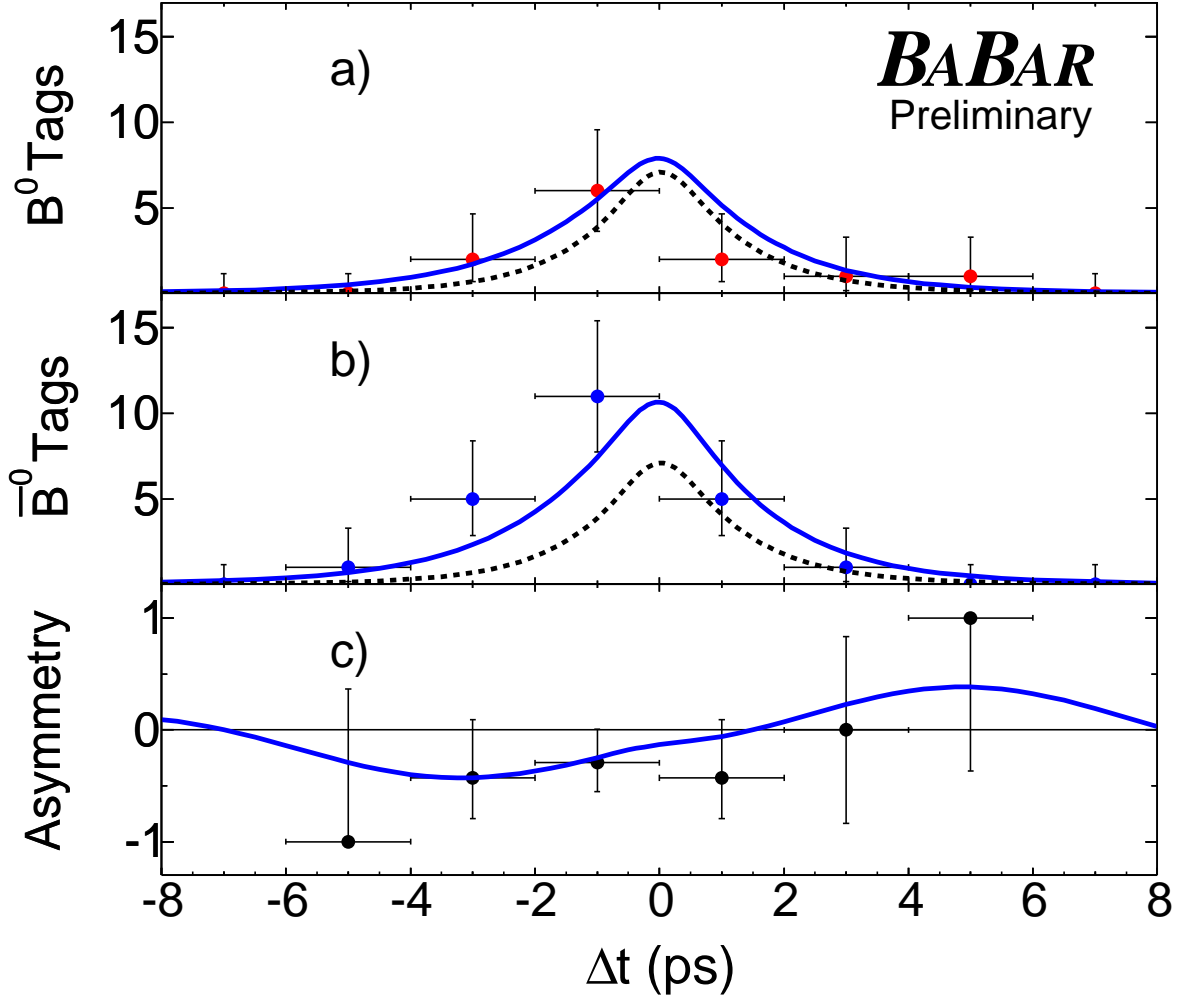


Figure 2: Plots (a) and (b) show the Δt distributions of B^0 - and \bar{B}^0 -tagged $B^0 \rightarrow K_S^0 \pi^0 \pi^0$ candidates. The solid lines refer to the fit for all events; the dashed lines correspond to the total background. Plot (c) shows the raw asymmetry (see text). A requirement is applied on the event likelihood to suppress background.

from repeated fits to simulated events for signal and backgrounds mixed together with the expected yields, and the uncertainty of the method is accounted for as systematic error.

We perform several consistency checks, including the measurement of the B^0 lifetime; we obtain $\tau_{B^0} = 1.25 \pm 0.47$ ps. We embed different B background samples from Monte-Carlo simulation in the data sample and obtain consistent yields and CP parameters from the fit. We use the PDFs to generate signal and background samples and find that 47% of the simulated experiments had likelihood values greater than the one obtained in the fit to the data.

Table 1: Sources of systematic uncertainty on S and C . The total error is obtained by summing the individual errors in quadrature.

Source	$\sigma(S)$	$\sigma(C)$
PDF parameterization for signal and background	0.05	0.11
Background fractions	0.03	0.02
CP in charmless B background	0.03	0.01
Vertex finding/Resolution function	0.02	0.05
Beam spot position	0.00	0.00
SVT alignment	0.02	0.01
Tag side interference	0.00	0.01
$\Delta m_d, \tau_B$	0.02	0.01
Fit Bias	0.04	0.02
Total systematic error	0.08	0.13

7 SUMMARY

We have presented a preliminary measurement of the CP violating asymmetries in $B^0 \rightarrow K_S^0 \pi^0 \pi^0$ ($K_S^0 \rightarrow \pi^+ \pi^-$) decays reconstructed from a sample of approximately 227 million $B\bar{B}$ pairs. From an unbinned extended maximum likelihood fit we obtain $S_{K_S^0 \pi^0 \pi^0} = 0.84 \pm 0.71$ (stat) ± 0.08 (syst) and $C_{K_S^0 \pi^0 \pi^0} = 0.27 \pm 0.52$ (stat) ± 0.13 (syst). The change in the log-likelihood when we fix the values of $-S_{K_S^0 \pi^0 \pi^0}$ to the average $\sin 2\beta$ measured in $b \rightarrow \bar{c}s$ modes, $\sin 2\beta = 0.725 \pm 0.037$ [22], and $C_{K_S^0 \pi^0 \pi^0}$ to zero, and re-fit the data sample is 2.5. The signal yield is consistent with our findings in the $B^0 \rightarrow K_S^0 \pi^+ \pi^-$ decay [23] assuming the dominant charmless final states are $f_0(980)K_S^0$, $K^*(892)\pi^0$, $K_0^*(1430)\pi^0$, and non-resonant $K_S^0 \pi^0 \pi^0$, and isospin symmetry.

8 ACKNOWLEDGMENTS

We are grateful for the extraordinary contributions of our PEP-II colleagues in achieving the excellent luminosity and machine conditions that have made this work possible. The success of this project also relies critically on the expertise and dedication of the computing organizations that support *BABAR*. The collaborating institutions wish to thank SLAC for its support and the kind hospitality extended to them. This work is supported by the US Department of Energy and National Science Foundation, the Natural Sciences and Engineering Research Council (Canada), Institute of High Energy Physics (China), the Commissariat à l’Energie Atomique and Institut National de Physique Nucléaire et de Physique des Particules (France), the Bundesministerium für Bildung und Forschung and Deutsche Forschungsgemeinschaft (Germany), the Istituto Nazionale di Fisica Nucleare (Italy), the Foundation for Fundamental Research on Matter (The Netherlands), the Research Council of Norway, the Ministry of Science and Technology of the Russian Federation, and the Particle Physics and Astronomy Research Council (United Kingdom). Individuals have received support from CONACyT (Mexico), the A. P. Sloan Foundation, the Research Corporation, and the Alexander von Humboldt Foundation.

References

- [1] Y. Grossman and M. P. Worah, Phys. Lett. B **395**, 241 (1997). M. Ciuchini, E. Franco, G. Martinelli, A. Masiero and L. Silvestrini, Phys. Rev. Lett. **79**, 978 (1997). D. London and A. Soni, Phys. Lett. B **407**, 61 (1997).
- [2] Unless explicitly stated, conjugate decay modes are assumed throughout this paper.
- [3] K. Abe *et al.* [Belle Collaboration], Phys. Rev. Lett. **91**, 261602 (2003).
- [4] B. Aubert *et al.* [BABAR Collaboration], Phys. Rev. Lett. **93**, 071801 (2004).
- [5] B. Aubert *et al.* [BABAR Collaboration], Branching Fraction and CP Asymmetries of $B^0 \rightarrow K_S^0 K_S^0 K_S^0$, hep-ex/0502013.
- [6] B. Aubert *et al.* [BABAR Collaboration], Phys. Rev. Lett. **91**, 161801 (2003).
- [7] B. Aubert *et al.* [BABAR Collaboration], Phys. Rev. Lett. **93**, 181805 (2004).
- [8] B. Aubert *et al.* [BABAR Collaboration], Phys. Rev. Lett. **94**, 041802 (2005).
- [9] B. Aubert *et al.* [BABAR Collaboration], Phys. Rev. Lett. **93**, 131805 (2004).
- [10] T. Gershon and M. Hazumi, Phys. Lett. B **596**, 163 (2004).
- [11] N. Cabibbo, Phys. Rev. Lett. **10**, 531 (1963); M. Kobayashi and T. Maskawa, Prog. Theor. Phys. **49**, 652 (1973).
- [12] Y. Grossman, Talk at Lepton-Photon 2003, hep-ph/0310229.
- [13] B. Aubert *et al.*, [BABAR Collaboration], Nucl. Instrum. Methods **A479**, 1-116 (2002).
- [14] PEP-II Conceptual Design Report, SLAC-R-418 (1993).
- [15] B. Aubert *et al.*, [BABAR Collaboration], Phys. Rev. Lett. **94**, 161803 (2005).
- [16] B. Aubert *et al.*, [BABAR Collaboration], Phys. Rev. D **66**, 032003 (2002).
- [17] S. Eidelmann *et al.* [PDG], Phys. Lett. B **592**, 1 (2004).
- [18] Broyden, C. G., Journal of the Institute for Mathematics and Applications, Vol. 6, pp 222-231, 1970; Fletcher, R., Computer Journal, Vol. 13, pp 317-322, 1970; Goldfarb, D., Mathematics of Computation, Vol. 24, pp 23-26, 1970; Shanno, D. F., Mathematics of Computation, Vol. 24, pp 647-656 1970.
- [19] B. Aubert *et al.*, [BABAR Collaboration], Phys. Rev. Lett. **94**, 181802 (2005).
- [20] W. D. Hulsbergen, Decay chain fitting with a Kalman filter, arXiv:physics/0503191.
- [21] O. Long, M. Baak, R.N. Cahn, and D. Kirkby, Phys. Rev. D **68**, 034010 (2003).
- [22] Heavy Flavor Averaging Group, Winter 2005 Results, <http://www.slac.stanford.edu/xorg/hfag/>

- [23] B. Aubert *et al.*, [BABAR Collaboration], Measurements of Neutral B Decay Branching Fractions to $K_S^0\pi^+\pi^-$ Final States and the Charge Asymmetry of $B^0 \rightarrow K^{*+}\pi^-$, hep-ex/0508013, *submitted to Phys.Rev.D Rapid Communications*.